

# Novel Signatures of Heavy Neutral Lepton at Muon Collider

Xue-Xin Zhang, Zhi-Long Han,<sup>\*</sup> Fei Huang,<sup>†</sup> and Honglei Li<sup>‡</sup>

*School of Physics and Technology, University of Jinan, Jinan, Shandong 250022, China*

(Dated: February 6, 2026)

The Higgs-strahlung process  $\ell^+\ell^- \rightarrow Zh$  is one of the most important production channels of the standard model Higgs boson  $h$  at the lepton colliders. The cross section reaches the maximum value slightly above the threshold  $\sqrt{s} \sim m_Z + m_h$ , and decreases as  $\sim 1/s$  at high energies. In the gauged extension models, the new gauge boson  $Z'$  and heavy Higgs boson  $H$  exist after the symmetry breaking. The heavy Higgs-strahlung process  $\ell^+\ell^- \rightarrow Z'H$  would also reach the maximum cross section around the threshold  $\sqrt{s} \sim m_{Z'} + m_H$ . Therefore, the future high energy lepton colliders, such as the TeV scale muon collider, are promising to probe this new process. If heavy neutral lepton  $N$  is introduced to generate the tiny neutrino masses via seesaw mechanism, novel signatures could arise from  $\mu^+\mu^- \rightarrow Z'H \rightarrow NN + NN \rightarrow 4\mu^\pm + 4J$  and  $\mu^+\mu^- \rightarrow Z'H \rightarrow \mu^+\mu^- + NN \rightarrow 3\mu^\pm\mu^\mp + 2J$ , where the fat-jets  $J$  come from the hadronic decay of  $W$  bosons. In this paper, we investigate the same-sign tetralepton signature  $4\mu^\pm + 4J$  and the same-sign trilepton signature  $3\mu^\pm\mu^\mp + 2J$  at the 3 TeV and 10 TeV muon collider.

---

<sup>\*</sup> [sps\\_hanzl@ujn.edu.cn](mailto:sps_hanzl@ujn.edu.cn)

<sup>†</sup> [sps\\_huangf@ujn.edu.cn](mailto:sps_huangf@ujn.edu.cn)

<sup>‡</sup> [sps\\_lihl@ujn.edu.cn](mailto:sps_lihl@ujn.edu.cn)

## I. INTRODUCTION

The observations of the tiny neutrino mass and mixing [1–3] are the direct evidence of physics beyond the standard model. Sub-eV scale neutrino mass can be naturally generated via the seesaw mechanism by introducing heavy neutral leptons  $N$  [4–7]. The promising lepton number violation signature, such as  $pp \rightarrow \ell^\pm N \rightarrow \ell^\pm \ell^\pm jj$  [8], is extensively studied in previous researches [9, 10]. Being singlets under the standard model symmetry, the production of heavy neutral leptons at colliders is governed by the mixing parameter with the light neutrinos  $V_{\ell N}$  [11–15]. However, the canonical seesaw prediction  $|V_{\ell N}|^2 \simeq m_\nu/m_N$  is heavily suppressed by the tiny neutrino mass, which can be hardly tested at colliders [16].

This motivates the gauge extension of the seesaw mechanism, such as the left-right symmetric model [17–19] and the gauged  $U(1)_{B-L}$  model [20–22]. Charged under the new gauge symmetry, the heavy neutral leptons have new interactions mediated by the new gauge bosons and new Higgs bosons, which could induce the lepton number violation signature at colliders that is independent of the mixing parameter  $V_{\ell N}$  [23–27]. However, with direct couplings to quarks, the new gauge bosons in the left-right symmetric and gauged  $U(1)_{B-L}$  models are tightly constrained by current LHC searches [28–31]. An alternative pathway is the leptophilic gauge symmetry, such as the  $U(1)_{L_\mu-L_\tau}$  symmetry [32, 33]. At LHC, the new gauge boson  $Z'$  can be produced by final state radiation from muon or tau flavor leptons, so the current searches are only sensitive to  $m_{Z'}$  less than 81 GeV [34, 35]. In the future, the proposed multi-TeV muon collider is promising to test the gauged  $U(1)_{L_\mu-L_\tau}$  symmetry [36–38].

Various signatures of heavy neutral lepton can be produced at the muon collider. With relatively large mixing parameter  $|V_{\ell N}|^2 > 10^{-6}$ , the promising signature is  $\mu^+ \mu^- \rightarrow N \nu \rightarrow \ell jj \nu$  [39–44]. Similar signature could also be induced by the dipole operator  $\bar{\nu} \sigma^{\mu\nu} N F_{\mu\nu}$  [45–47]. Lepton number violation signature can originate from the vector boson scattering process  $W^\pm Z/\gamma \rightarrow \ell^\pm N \rightarrow \ell^\pm \ell^\pm jj$  [48–50], and from the associated production process  $\mu^+ \mu^- \rightarrow N W^\pm \ell^\mp \rightarrow W^\pm W^\pm \ell^\mp \ell^\mp$  [51]. At the same sign muon collider, heavy neutral lepton will contribute to the  $t$ -channel process  $\mu^+ \mu^+ \rightarrow W^+ W^+$  [52–54]. Meanwhile, lepton number violation signature from heavy neutral lepton pair production  $NN \rightarrow \ell^\pm \ell^\pm 4j$  can be mediated by the new gauge boson  $Z'$  [55–57], the axion-like particle  $a$  [58], and the Higgs bosons  $H^\pm/h/H$  [59–61], which is not suppressed by the seesaw induced mixing parameter.

It is well known that the Higgs-strahlung process  $\ell^+ \ell^- \rightarrow Z h$  is the most important production channel of the standard model Higgs  $h$  at the lepton colliders [62, 63]. The cross section reaches the maximum value slightly above the threshold  $\sqrt{s} \sim m_Z + m_h$ , and decreases as  $1/s$  at high energies. Therefore, the dominant production channel of Higgs  $h$  becomes the vector boson fusion process  $\mu^+ \mu^- \rightarrow \nu_\mu \bar{\nu}_\mu h$  at the TeV scale muon collider [64]. In the gauged  $U(1)$  extension of seesaw models, the new gauge boson  $Z'$  and

heavy Higgs  $H$  exist after the symmetry breaking. The new Higgs-strahlung process  $\mu^+\mu^- \rightarrow Z'H$  would reach the maximum cross section around the threshold  $\sqrt{s} \sim m_{Z'} + m_H$  [65]. Hence, the multi-TeV scale muon collider is quite promising to probe new  $Z'$  and  $H$  above the electroweak scale [66]. Cascade decays of the new particles could generate novel signatures as  $\mu^+\mu^- \rightarrow Z'H \rightarrow NN + NN \rightarrow 4\mu^\pm + 4J$  and  $\mu^+\mu^- \rightarrow Z'H \rightarrow \mu^+\mu^- + NN \rightarrow 3\mu^\pm\mu^\mp + 2J$ , where the fat-jets  $J$  come from the hadronic decay of  $W$  bosons. In this paper, we investigate the same-sign tetralepton signature  $4\mu^\pm + 4J$  and the same-sign trilepton signature  $3\mu^\pm\mu^\mp + 2J$  at the 3 TeV and 10 TeV muon collider in the less constrained gauged  $U(1)_{L_\mu-L_\tau}$  symmetry.

This paper is organized as follows. In Section II, we review the gauged  $U(1)_{L_\mu-L_\tau}$  symmetry extended seesaw model. The decay properties of the new gauge boson  $Z'$  and heavy Higgs  $H$  are studied in Section III. The cross section of the heavy Higgs-strahlung at muon collider  $\mu^+\mu^- \rightarrow Z'H$  is calculated in Section IV. The novel same-sign tetralepton signature  $4\mu^\pm + 4J$  and same-sign trilepton  $3\mu^\pm\mu^\mp + 2J$  are investigated in Section V and Section VI, respectively. Finally, the conclusion is in Section VII.

## II. THE MODEL

Among various gauged extensions of the standard model [67, 68], the  $U(1)_{L_\mu-L_\tau}$  symmetry is less constrained at present due to the lack of direct couplings of  $Z'$  to quarks and electron. While the muon collider is promising to test this  $U(1)_{L_\mu-L_\tau}$  symmetry. The gauged  $U(1)_{L_\mu-L_\tau}$  seesaw model contains three heavy neutral leptons ( $N_e, N_\mu, N_\tau$ ). A scalar singlet  $S$  with  $U(1)_{L_\mu-L_\tau}$  charge +1 breaks the symmetry spontaneously. The new kinetic terms are [69, 70]

$$\mathcal{L} \supset -\frac{1}{4}F'_{\mu\nu}F'^{\mu\nu} - \frac{\epsilon}{2}F'_{\mu\nu}F^{\mu\nu} + |D_\mu S|^2, \quad (1)$$

where  $F'_{\mu\nu}$  and  $F_{\mu\nu}$  are the field strength of the  $U(1)_{L_\mu-L_\tau}$  and  $U(1)_Y$  symmetry.  $D_\mu = \partial_\mu - ig'Z'_\mu$  is the covariant derivative with  $g'$  being the  $L_\mu - L_\tau$  gauge coupling constant. The second term induces the mixing between the standard model gauge boson  $Z$  and new gauge boson  $Z'$  [71, 72]. For simplicity, we assume vanishing kinetic mixing  $\epsilon = 0$  in the following studies. After  $S$  obtains nonzero vacuum expectation value  $v_S$ ,  $Z'$  boson develops mass as [73]

$$m_{Z'} = g'v_S. \quad (2)$$

The interactions of the new boson  $Z'$  with fermions are

$$\mathcal{L} \supset g'(\bar{\mu}\gamma^\mu\mu - \bar{\tau}\gamma^\mu\tau + \bar{\nu}_\mu\gamma^\mu P_L\nu_\mu - \bar{\nu}_\tau\gamma^\mu P_L\nu_\tau + \bar{N}_\mu\gamma^\mu P_R N_\mu - \bar{N}_\tau\gamma^\mu P_R N_\tau)Z'_\mu. \quad (3)$$

The scalar potential of the Higgs doublet  $\Phi$  and singlet  $S$  under the  $U(1)_{L_\mu - L_\tau}$  symmetry is [66]

$$V = -\mu_\Phi^2 \Phi^\dagger \Phi - \mu_S^2 S^* S + \lambda_\Phi (\Phi^\dagger \Phi)^2 + \lambda_S (S^* S)^2 + \lambda_{\Phi S} (\Phi^\dagger \Phi)(S^* S). \quad (4)$$

After the spontaneous symmetry breaking, the scalars can be denoted as

$$\Phi = \begin{pmatrix} 0 \\ \frac{v_0 + \phi^0}{\sqrt{2}} \end{pmatrix}, S = \frac{v_s + s^0}{\sqrt{2}}. \quad (5)$$

The squared mass matrix for the CP-even scalar bosons is

$$M^2(\phi^0, s^0) = \begin{pmatrix} 2\lambda_\Phi v_0^2 & \lambda_{\Phi S} v_0 v_s \\ \lambda_{\Phi S} v_0 v_s & 2\lambda_S v_s^2 \end{pmatrix}, \quad (6)$$

which can be diagonalized by an orthogonal transformation as

$$\begin{pmatrix} h \\ H \end{pmatrix} = \begin{pmatrix} \cos \alpha & -\sin \alpha \\ \sin \alpha & \cos \alpha \end{pmatrix} \begin{pmatrix} \phi^0 \\ s^0 \end{pmatrix}, \tan(2\alpha) = \frac{\lambda_{\Phi S} v_0 v_s}{\lambda_S v_s^2 - \lambda_\Phi v_0^2}. \quad (7)$$

The corresponding masses for the two physical Higgs states  $h, H$  are

$$m_h^2 = \lambda_\Phi v_0^2 + \lambda_S v_s^2 - \sqrt{(\lambda_\Phi v_0^2 - \lambda_S v_s^2)^2 + (\lambda_{\Phi S} v_0 v_s)^2}, \quad (8)$$

$$m_H^2 = \lambda_\Phi v_0^2 + \lambda_S v_s^2 + \sqrt{(\lambda_\Phi v_0^2 - \lambda_S v_s^2)^2 + (\lambda_{\Phi S} v_0 v_s)^2}. \quad (9)$$

In this paper, we regard  $h$  as the standard model Higgs. Under the current LHC constraints,  $\sin \alpha \lesssim 0.1$  should be satisfied for  $m_H$  above the electroweak scale [74]. To satisfy this constraint, we assume  $\sin \alpha = 0$  for simplicity.

The Yukawa interactions and mass terms in the minimal scenario are given by [75]

$$\begin{aligned} \mathcal{L} \supset & -y_e \bar{L}_e \tilde{\Phi} N_e - y_\mu \bar{L}_\mu \tilde{\Phi} N_\mu - y_\tau \bar{L}_\tau \tilde{\Phi} N_\tau - \frac{1}{2} M_{ee} \bar{N}_e^c N_e \\ & - y_{e\mu} S^* \bar{N}_e^c N_\mu - y_{e\tau} S \bar{N}_e^c N_\tau - M_{\mu\tau} \bar{N}_\mu^c N_\tau + \text{h.c.}, \end{aligned} \quad (10)$$

where  $L_e, L_\mu, L_\tau$  are the lepton doublets, and  $\tilde{\Phi} = i\tau_2 \Phi^*$ . The resulting Dirac neutrino mass matrix and heavy neutral lepton mass matrix are

$$M_D = \begin{pmatrix} \frac{y_e v_0}{\sqrt{2}} & 0 & 0 \\ 0 & \frac{y_\mu v_0}{\sqrt{2}} & 0 \\ 0 & 0 & \frac{y_\tau v_0}{\sqrt{2}} \end{pmatrix}, \quad M_N = \begin{pmatrix} M_{ee} & \frac{y_{e\mu} v_s}{\sqrt{2}} & \frac{y_{e\tau} v_s}{\sqrt{2}} \\ \frac{y_{e\mu} v_s}{\sqrt{2}} & 0 & M_{\mu\tau} \\ \frac{y_{e\tau} v_s}{\sqrt{2}} & M_{\mu\tau} & 0 \end{pmatrix}. \quad (11)$$

Light neutrino masses are generated via the type-I seesaw mechanism

$$M_\nu \simeq -M_D M_N^{-1} M_D^T. \quad (12)$$

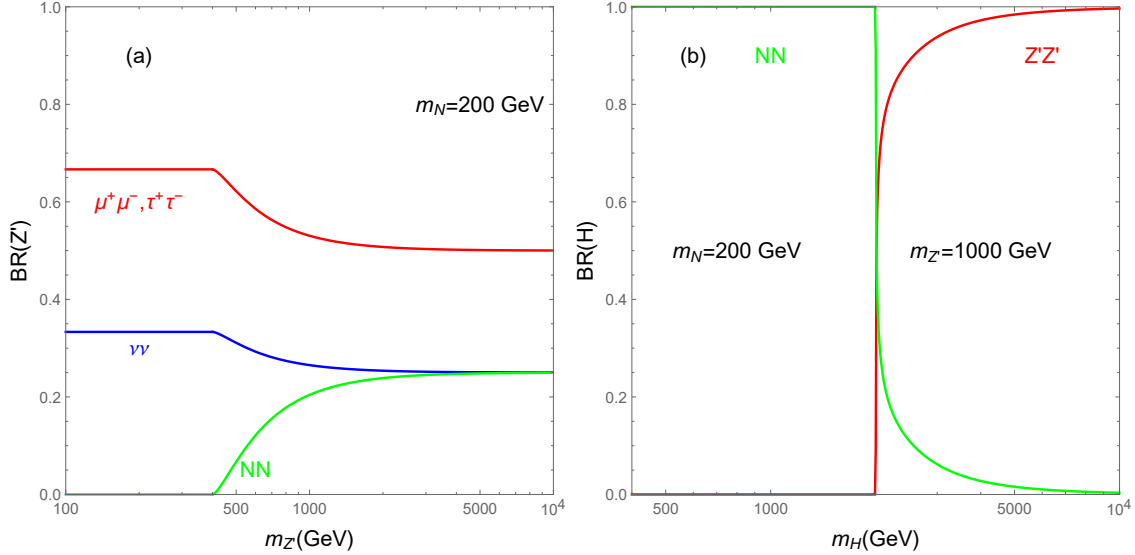


FIG. 1. Branching ratio of new gauge boson  $Z'$  in panel (a) and heavy Higgs  $H$  in panel (b). We have set  $m_N = 200 \text{ GeV}$  in panel (a). Meanwhile,  $m_{Z'}$  is fixed to  $1000 \text{ GeV}$  in panel (b).

### III. DECAY PROPERTIES

In this section, we study the decay properties of the new gauge boson  $Z'$  and heavy Higgs  $H$ . The partial decay widths of  $Z'$  are calculated as

$$\Gamma(Z' \rightarrow \ell^+ \ell^-) = \frac{g'^2}{12\pi} m_{Z'}, \quad (13)$$

$$\Gamma(Z' \rightarrow \nu_\ell \nu_\ell) = \frac{g'^2}{24\pi} m_{Z'}, \quad (14)$$

$$\Gamma(Z' \rightarrow NN) = \frac{g'^2}{24\pi} m_{Z'} \left(1 - 4 \frac{m_N^2}{m_{Z'}^2}\right). \quad (15)$$

In the decoupling limit  $\sin \alpha = 0$ , there are only two viable decay modes of the heavy Higgs, i.e.,  $H \rightarrow NN$  and  $H \rightarrow Z'Z'$  [73]. The corresponding decay widths are

$$\Gamma(H \rightarrow NN) = \frac{m_N^2 m_H}{4\pi v_s^2} \left(1 - \frac{4m_N^2}{m_H^2}\right)^{3/2}, \quad (16)$$

$$\Gamma(H \rightarrow Z'Z') = \frac{m_H^3}{32\pi v_s^2} \left(1 - \frac{4m_{Z'}^2}{m_H^2} + \frac{12m_{Z'}^4}{m_H^4}\right) \left(1 - \frac{4m_{Z'}^2}{m_H^2}\right)^{1/2}. \quad (17)$$

In Figure 1, we show the numerical results for the branching ratio of the new gauge boson  $Z'$  and heavy Higgs  $H$ . Decays of  $Z'$  into charged lepton pair  $\mu^+\mu^-$ ,  $\tau^+\tau^-$  are the dominant channel. In the limit of  $m_N \ll m_{Z'}$ , we approximately have  $BR(Z' \rightarrow \nu\nu) \simeq BR(Z' \rightarrow NN) \simeq 0.25$ . For the heavy Higgs, the  $H \rightarrow NN$  is the only decay mode when  $m_H < 2m_{Z'}$ . Once kinematically allowed, the  $H \rightarrow Z'Z'$

quickly becomes the dominant decay mode, as  $\Gamma(H \rightarrow Z'Z')$  is proportional to  $m_H^3$  while  $\Gamma(H \rightarrow NN)$  is proportional to  $m_H$ .

#### IV. HEAVY HIGGS-STRÄHLUNG AT MUON COLLIDER

The novel lepton number violation signatures are induced through the heavy Higgs-strahlung process at the muon collider

$$\mu^+\mu^- \rightarrow Z'H. \quad (18)$$

The cross section of this heavy Higgs-strahlung is calculated as

$$\sigma(\mu^+\mu^- \rightarrow Z'H) = \frac{g'^4}{48\pi s^2} \frac{\lambda(s, m_{Z'}^2, m_H^2) + 12sm_{Z'}^2}{(s - m_{Z'}^2)^2 + m_{Z'}^2\Gamma_{Z'}^2} \sqrt{\lambda(s, m_{Z'}^2, m_H^2)}, \quad (19)$$

where  $\Gamma_{Z'}$  is the total decay width of  $Z'$ , and the function  $\lambda(x, y, z)$  is defined as

$$\lambda(x, y, z) = x^2 + y^2 + z^2 - 2xy - 2xz - 2yz. \quad (20)$$

In Figure 2, we depict the cross section of heavy Higgs-strahlung for some benchmark scenarios. In panel (a) of Figure 2, we report the cross section as a function of the collision energy for the scenario with  $m_{Z'} = m_H = 1000(3000)$  GeV. It is clear that the cross section quickly reaches the maximum value when the collision energy is slightly above the threshold  $\sqrt{s} > m_{Z'} + m_H$ , and decreases as  $\sim g'^4/s$  at high energies.

In panels (b) to (d) of Figure 2, we fix the collision energy of the muon collider to 3 TeV and 10 TeV [76, 77] for illustration. The scenario with  $m_{Z'} = m_H$  is shown in panel (b) of Figure 2. We find that apart from the threshold region, the cross section of  $\mu^+\mu^- \rightarrow Z'H$  increases as  $m_{Z'} (= m_H)$  becomes larger. Maximum cross section is obtained with  $m_{Z'} = m_H \sim 0.4\sqrt{s}$  in this scenario. Typically, for  $g' \gtrsim 0.1$ , the cross section of  $\mu^+\mu^- \rightarrow Z'H$  is larger than  $10^{-3}$  fb, which is promising with an integrated luminosity larger than  $1 \text{ ab}^{-1}$  at the muon collider. Meanwhile, with a relatively larger cross section for a fixed value of  $g'$ , the 3 TeV muon collider is actually more promising than the 10 TeV muon collider to test  $Z'$  and  $H$  below the TeV scale.

In panel (c) of Figure 2, we fix  $m_H = 1000$  GeV to show the impact of  $m_{Z'}$ . Compared to the scenario  $m_{Z'} = m_H$ , increasing  $m_{Z'}$  alone would greatly enhance the cross section near the threshold, which is due to the cancellation in the denominator of Equation (19). On the other hand, increasing  $m_H$  alone would lead to a smaller cross section, which is shown in panel (d) of Figure 2.

With vanishing Higgs mixing angle  $\sin \alpha = 0$ , the decay  $H \rightarrow NN$  is the only viable channel of heavy Higgs with  $m_{Z'} = m_H$ . When the new gauge boson also decays into heavy neutral leptons  $Z' \rightarrow NN$ ,

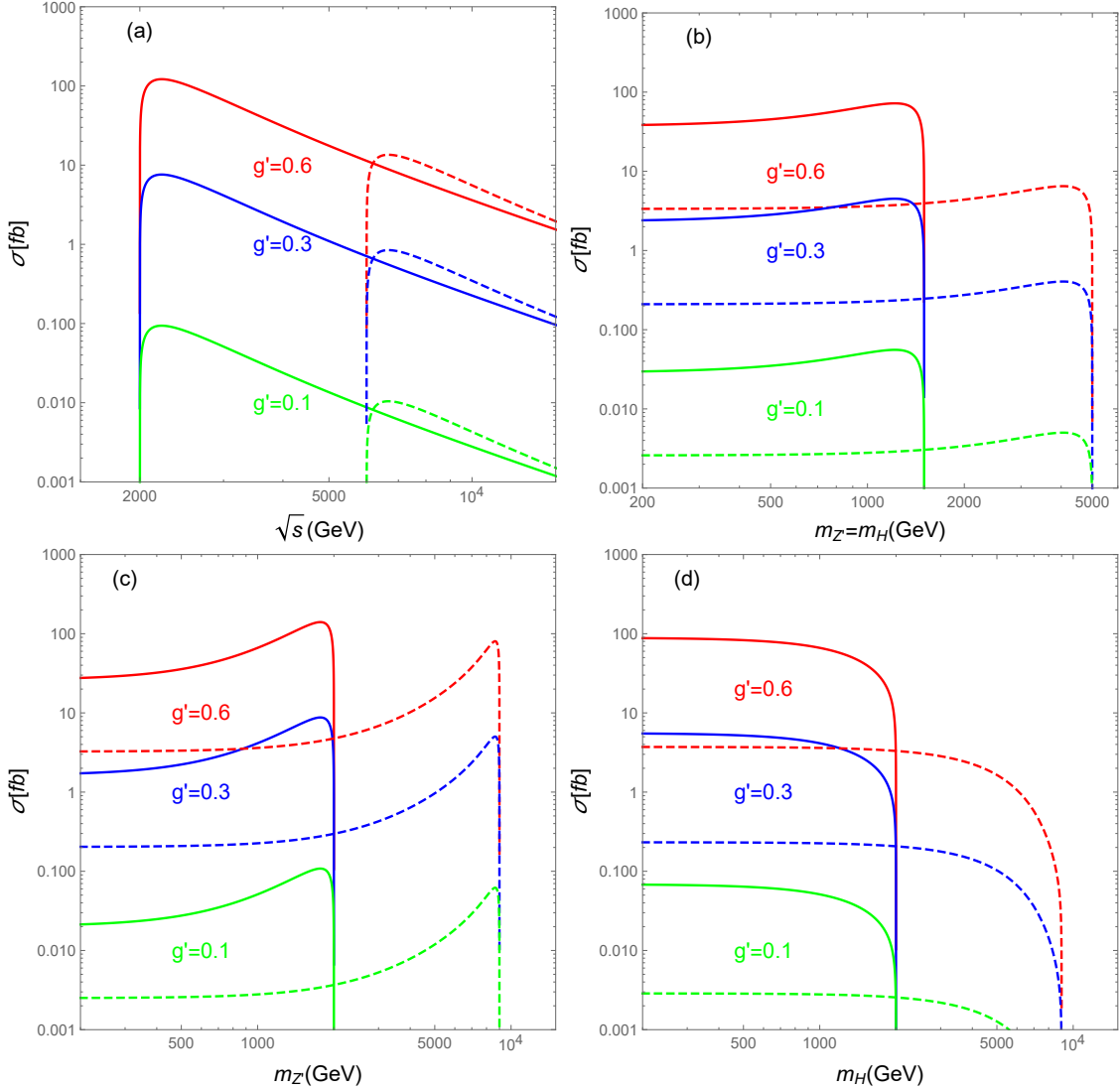


FIG. 2. Cross section of the heavy Higgs-strahlung at muon collider. The red, blue, and green lines are the results for  $g' = 0.6, 0.3, 0.1$ , respectively. In panel (a), the solid (dashed) lines are the results for  $m_{Z'} = m_H = 1000$  (3000) GeV. In panel (b), we assume  $m_{Z'} = m_H$ . In panel (c), we fix  $m_H = 1000$  GeV. In panel (d), we fix  $m_{Z'} = 1000$  GeV. Solid (dashed) lines in panel (b)-(d) are the results at the 3 (10) TeV muon collider.

there are a total of four heavy neutral leptons in the final states. Further decay of the heavy neutral leptons could induce various interesting signatures. Considering the fully visible decay mode  $N \rightarrow \ell^\pm W^\mp \rightarrow \ell^\pm J$ , the promising signatures from  $4N$  are

$$4N \rightarrow 4\ell^\pm + 4J, \quad (21)$$

$$\rightarrow 3\ell^\pm + \ell^\mp + 4J, \quad (22)$$

$$\rightarrow 2\ell^+ + 2\ell^- + 4J. \quad (23)$$

On the other hand, when considering the leptonic decay of the new gauge boson  $Z' \rightarrow \ell^+ \ell^-, \nu_\ell \nu_\ell$ , the interesting signatures would be

$$\ell^+ \ell^- NN \rightarrow \ell^+ \ell^- + \ell^\pm J + \ell^\pm J \rightarrow 3\ell^\pm + \ell^\mp + 2J \quad (24)$$

$$\rightarrow \ell^+ \ell^- + \ell^+ J + \ell^- J \rightarrow 2\ell^+ + 2\ell^- + 2J \quad (25)$$

$$\nu_\ell \nu_\ell NN \rightarrow \nu_\ell \nu_\ell + \ell^\pm J + \ell^\pm J \rightarrow 2\ell^\pm + 2J + \cancel{E}_T \quad (26)$$

$$\rightarrow \nu_\ell \nu_\ell + \ell^+ J + \ell^- J \rightarrow \ell^+ \ell^- + 2J + \cancel{E}_T \quad (27)$$

An investigation of all these signatures from the cascade  $Z' H$  decay is beyond the scope of this paper. In the following, we study the novel same-sign tetralepton signature  $4\ell^\pm + 4J$  and the same-sign trilepton signature  $3\ell^\pm \ell^\mp + 2J$ . These two lepton number violation signatures have a relatively clean background process. Meanwhile, the heavy resonances  $Z'$ ,  $H$ , and  $N$  can all be reconstructed as we consider the fully visible decay chain.

## V. SAME-SIGN TETRALEPTON SIGNATURE

In this paper, we consider a muon-flavored heavy neutral lepton for illustration, i.e.,  $V_{\mu N} \neq 0, V_{e N} = V_{\tau N} = 0$ . For simplicity, we assume  $m_{Z'} = m_H$  in the following studies. The full process of the same-sign tetralepton signature is

$$\mu^+ \mu^- \rightarrow Z' H \rightarrow NN + NN \rightarrow 4\mu^\pm + 4W^\mp \rightarrow 4\mu^\pm + 4J, \quad (28)$$

where the fat-jets  $J$  come from the hadronic decay of  $W$  bosons. There are no irreducible backgrounds of this novel signature. In the following studies, we assume one background event  $N_B = 1$  for a conservative estimation.

In the simulation, we use the **FeynRules** package [78] to implement the  $U(1)_{L_\mu - L_\tau}$  extension of the type-I seesaw model. We then use **Madgraph5\_aMC@NLO** [79] to generate the leading order signal events at the parton level. After this, **Pythia8** [80] is used to do parton showering and hadronization, and the detector simulation is performed by **Delphes3** [81] with the corresponding muon collider card. The fat-jets are reconstructed by using the Valencia algorithm [82] with  $R = 1.2$ .

Since this signature is background free, we apply the default pre-selection cuts of **Delphes3**:

$$P_T(\mu) > 20 \text{ GeV}, |\eta(\mu)| < 2.5, P_T(J) > 50 \text{ GeV}, |\eta(J)| < 2.5, \quad (29)$$

The distributions of some variables for the signal at the 3 TeV and 10 TeV muon collider after the pre-selection cuts are shown in Figure 3. It is obvious that with a larger heavy neutral lepton mass  $m_N$ , the

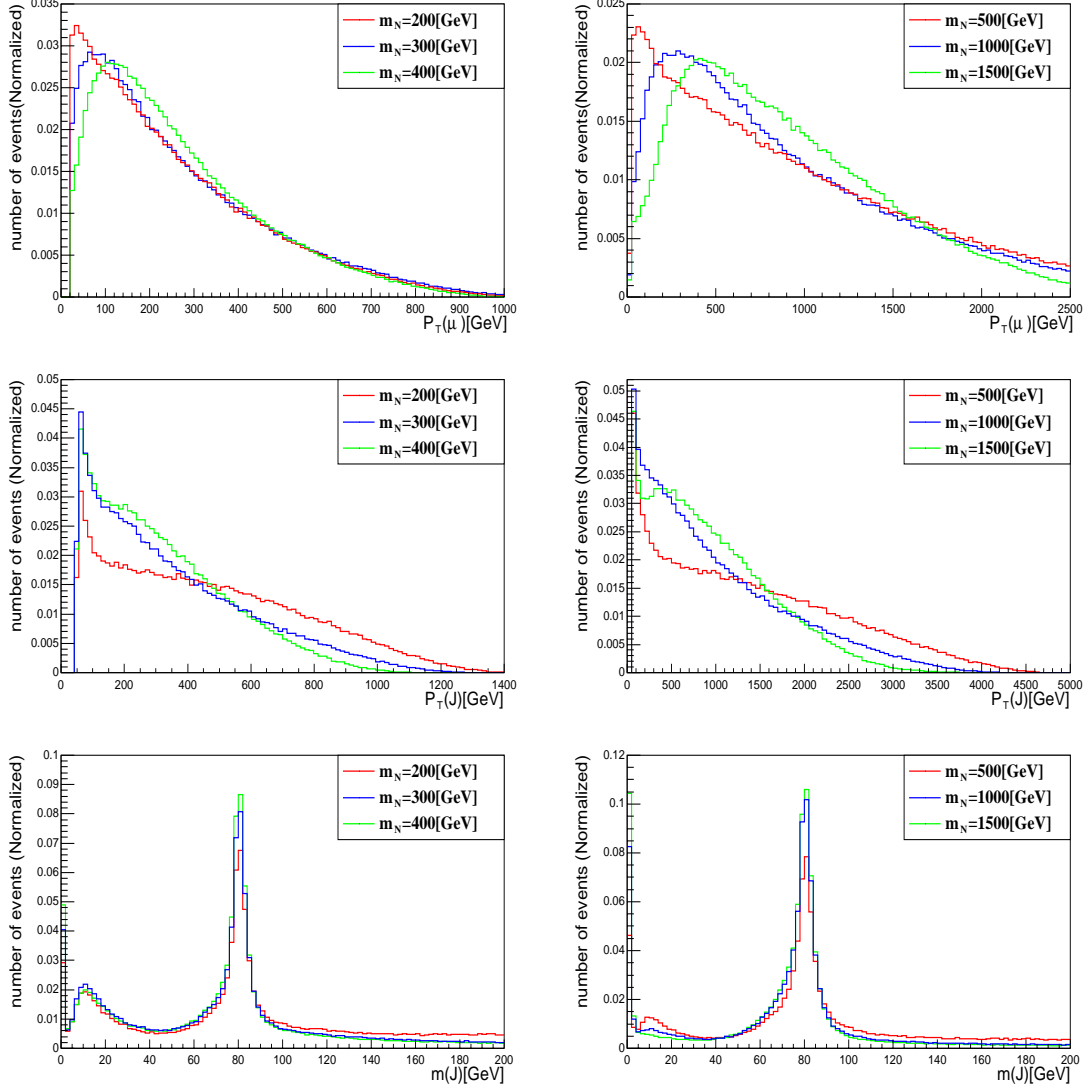


FIG. 3. Normalized distributions of muon transverse momentum  $P_T(\mu)$ , fat-jet transverse momentum  $P_T(J)$ , and invariant mass of fat-jet  $m_J$ . Left panels are the results of 3 TeV, and right panels are the results of 10 TeV. During the simulation of these plots, we have assumed the relation  $m_{Z'} = m_H = 3m_N$  for illustration.

transverse momentum of the final state muon  $P_T(\mu)$  tends to be more energetic. We also report that the Valencia fat-jet algorithm is more efficient for reconstructing fat-jet from heavier  $N$ .

In order to reconstruct the heavy resonance through the decay chain  $H/Z' \rightarrow NN \rightarrow \mu^\pm\mu^\pm JJ$ , it is enough to require two fat-jets. For the gauge boson, the purely leptonic channel  $Z' \rightarrow \mu^+\mu^-$  is more promising due to higher detection efficiency, which will be considered in Section VI. The same-sign tetralepton signature is then selected as

$$N(\mu^\pm) = 4, N(J) \geq 2. \quad (30)$$

$\mu^+ \mu^- \rightarrow 4\mu^\pm + 4J$		Pre-Selection (fb)	After Selection (fb)	Significance	$5\sigma$ Luminosity (fb $^{-1}$ )
3 TeV	$m_N = 200$ GeV	$7.33 \times 10^{-2}$	$3.09 \times 10^{-2}$	12.6	269.3
	$m_N = 300$ GeV	$8.80 \times 10^{-2}$	$4.84 \times 10^{-2}$	17.0	171.9
	$m_N = 400$ GeV	$1.01 \times 10^{-1}$	$5.56 \times 10^{-2}$	18.6	149.7
10 TeV	$m_N = 500$ GeV	$5.56 \times 10^{-3}$	$2.35 \times 10^{-3}$	10.5	3541
	$m_N = 1000$ GeV	$7.82 \times 10^{-3}$	$4.21 \times 10^{-3}$	15.5	1978
	$m_N = 1500$ GeV	$8.07 \times 10^{-3}$	$4.33 \times 10^{-3}$	15.8	1925

TABLE I. Results for the benchmark points at the muon collider, where we have fixed the relation  $m_{Z'} = m_H = 3m_N$  and  $g' = 0.6$ . The significance is calculated with an integrated luminosity of 1 (10) ab $^{-1}$  for the 3 TeV (10 TeV) muon collider.

where at least two fat-jets are required in order to keep more signal events during the analysis. According to Figure 3, we also require the fat-jet mass within the range of

$$50 \text{ GeV} < m_J < 110 \text{ GeV}, \quad (31)$$

to make sure it's coming from the decay of the  $W$  boson. Since this signature is background free, no further cut is applied.

In Table I, we show the results for some benchmark points at the muon collider. The significance is calculated as [83]

$$S = \sqrt{2 \left[ (N_S + N_B) \ln \left( 1 + \frac{N_S}{N_B} \right) - N_S \right]}, \quad (32)$$

where  $N_S$  and  $N_B$  are the events number of the signal and background, respectively. The benchmark points for the 3 TeV muon collider are selected as  $m_N = 200, 300$ , and  $400$  GeV with the mass relation  $m_{Z'} = m_H = 3m_N$  and  $g' = 0.6$ . After all selection cuts, the cross sections are  $3.09 \times 10^{-2}$  fb,  $4.84 \times 10^{-2}$  fb, and  $5.56 \times 10^{-2}$  fb for  $m_N = 200$  GeV, 300 GeV, and 400 GeV, respectively. The cross sections clearly increase as  $m_N$  becomes larger, which means that the muon collider is more sensitive to heavier  $N$ . With an integrated luminosity of 1 ab $^{-1}$  at the 3 TeV muon collider, the significance could reach 12.6, 17.0, and 18.6 for  $m_N = 200$  GeV, 300 GeV, and 400 GeV. The benchmark point with  $m_N = 200$  GeV can be discovered with the luminosity of 269.3 fb $^{-1}$ . Meanwhile, it is enough with 200 fb $^{-1}$  to discover those benchmarks with  $m_N = 300$  GeV and 400 GeV.

As shown in Figure 2, the cross section of the heavy Higgs-strahlung  $\mu^+ \mu^- \rightarrow Z' H$  at the 3 TeV muon collider is actually larger than it at the 10 TeV muon collider, so the 3 TeV muon collider is more promising to probe relatively light resonances. We then choose the benchmark points as  $m_N = 500$  GeV, 1000 GeV,

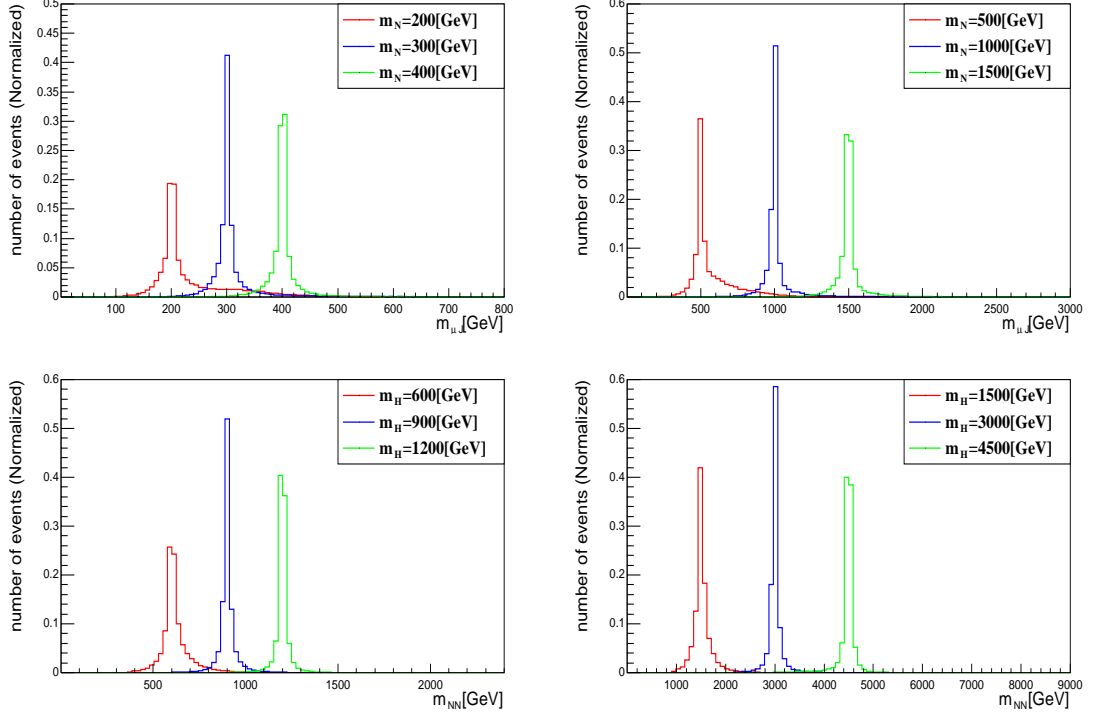


FIG. 4. Normalized distributions of invariant mass of muon and fat-jet  $m_{\mu J}$  and invariant mass of two reconstructed heavy neutral lepton  $m_{NN}$ . Left panels are the results of 3 TeV, and right panels are the results of 10 TeV. The relation  $m_{Z'} = m_H = 3m_N$  is also assumed.

and 1500 GeV with  $m_{Z'} = m_H = 3m_N$  for the 10 TeV muon collider. The production cross sections of these 10 TeV benchmarks are approximately an order of magnitude smaller than those of the 3 TeV ones. After all selection cuts, the cross sections are  $2.35 \times 10^{-3}$  fb,  $4.21 \times 10^{-3}$  fb, and  $4.33 \times 10^{-3}$  fb for  $m_N = 500$  GeV, 1000 GeV, and 1500 GeV, which leads to the significance of 10.5, 15.5, and 15.8 with an integrated luminosity of  $10 \text{ ab}^{-1}$ , respectively. Therefore, thanks to much higher integrated luminosity, the TeV-scale new particles are also within the reach of the 10 TeV muon collider through the same-sign tetralepton signature.

The masses of all new particles can be reconstructed by the final states of the same-sign tetralepton signature. According to the heavy neutral lepton decay  $N \rightarrow \mu^\pm J$ , its mass is determined by the invariant mass of one muon and one fat-jet  $m_{\mu J}$ . With multi muons and fat-jets in the signature, we reconstruct the heavy neutral lepton masses by minimizing [55]

$$\chi_N^2 = \sum_{i,j} (m_{\mu_i^\pm J_j} - m_N)^2 \quad (33)$$

for all detected muons and fat-jets. The reconstructed heavy neutral lepton masses of the benchmark points

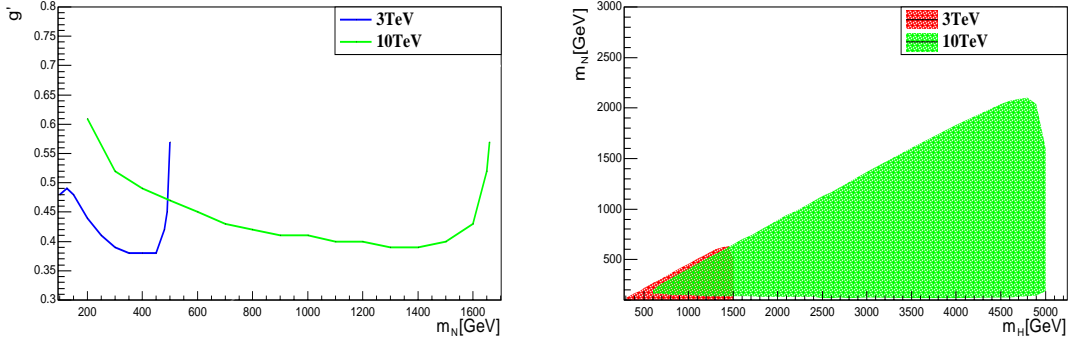


FIG. 5. Left: The  $5\sigma$  discovery region of the same-sign tetralepton signature in the  $g' - m_N$  plane, where we fix  $m_{Z'} = m_H = 3m_N$ . Right: The  $5\sigma$  discovery region of the same-sign tetralepton signature in the  $m_N - m_H$  plane, where we fix  $m_{Z'} = m_H$  and  $g' = 0.6$ .

are shown in Figure 4. To obtain the mass of heavy Higgs or gauge boson through the decay  $H/Z' \rightarrow NN$ , we can consider the invariant mass of the reconstructed heavy neutral leptons. To determine the correct origin of the heavy neutral leptons, the heavy Higgs or gauge boson is reconstructed by minimizing

$$\chi_H^2 = \sum_{i,j} (m_{N_i N_j} - m_H)^2 \quad (34)$$

for all reconstructed heavy neutral leptons. It should be mentioned that Equation (34) is only suitable for the simplified scenario with  $m_H = m_{Z'}$ . The results are shown in Figure 4, where only one resonance appears for a certain benchmark point.

Based on the above analysis, we then investigate the promising region of the same-sign tetralepton signature. In the left panel of Figure 5, we show the  $5\sigma$  discovery region in the  $g' - m_N$  plane, where we fix the relation  $m_{Z'} = m_H = 3m_N$  for illustration. With growing production cross section, the discovery reach of  $g'$  typically decreases as  $m_N$  becomes larger before the kinematic threshold. Obviously, the 3 TeV muon collider is more promising to probe the region with  $m_N \lesssim 500$  GeV. The 3 TeV muon collider could discover a large part of the regime with  $g' \gtrsim 0.38$  for the electroweak scale heavy neutral lepton. With higher integrated luminosity, the 10 TeV muon collider would unravel the parameter space with  $g' \gtrsim 0.4$ .

In the right panel of Figure 5, we depict the sensitive region in the  $m_N - m_H$  plane for the scenario of  $m_{Z'} = m_H$  and  $g' = 0.6$ . We report that the 3 TeV muon collider could detect the parameter space with  $400 \text{ GeV} \lesssim m_H \lesssim 1500 \text{ GeV}$ , which covers a large part of the kinematically allowed region. The 10 TeV muon collider could probe the regime of  $600 \text{ GeV} \lesssim m_H \lesssim 5000 \text{ GeV}$ . We find that the 10 TeV muon collider is not promising to detect  $m_N$  below about 150 GeV, which is mainly due to the non-isolation of the muon from the jet in the highly boosted heavy neutral lepton decays. Close to the threshold region with

$m_{Z'} = m_H \sim 2m_N$ , the branching ratio of  $Z' \rightarrow NN$  is also suppressed, so the same-sign tetralepton signature is not promising in such a region either.

Although the same-sign tetralepton signature  $4\mu^\pm + 4J$  is the most exotic signal, it should not be the most promising one to discover the heavy neutral leptons  $N$ , new gauge boson  $Z'$ , and heavy Higgs  $H$ . For instance, when combining all the visible final states of  $4N$  without distinguishing the specific charge of muon, the cross section of the tetralepton signature  $4\mu + 4J$  is theoretically eight times larger than that of the same-sign one  $4\mu^\pm + 4J$ . With a much larger cross section, the tetralepton signature might probe a larger parameter space by properly dealing with the backgrounds.

## VI. SAME-SIGN TRILEPTON SIGNATURE

As shown in Figure 1, the leptonic  $Z' \rightarrow \mu^+\mu^-$  is the dominant decay mode. This leptonic decay  $Z' \rightarrow \mu^+\mu^-$  also has much higher detection efficiency than the  $Z' \rightarrow NN$  mode, so the same-sign trilepton signature is expected to be more promising than the same-sign tetralepton signature. In this scenario, lepton number violation is only from the heavy Higgs decay. The same-sign trilepton signature is generated via the process

$$\mu^+\mu^- \rightarrow Z'H \rightarrow \mu^+\mu^- + NN \rightarrow \mu^+\mu^- + 2\mu^\pm + 2W^\mp \rightarrow 3\mu^\pm\mu^\mp + 2J. \quad (35)$$

We notice that the cross section of the background for the same-sign dilepton signature  $2\mu^\pm + 2J$  after certain selection cuts is at the order of  $\mathcal{O}(10^{-3})$  fb [56]. With two more muons in the final states, the cross section of the background for the same-sign trilepton signature  $3\mu^\pm\mu^\mp + 2J$  is roughly at the order of  $\mathcal{O}(10^{-3}) \times \alpha_{\text{em}} \sim 10^{-5}$  fb. The resulting background event is less than one even with  $10 \text{ ab}^{-1}$  data at the muon collider. For illustration, we also assume one background event  $N_B = 1$  in this section to calculate the significance.

We employ the same pre-selection cuts in Equation (29) in this section. The same-sign trilepton signature is then extracted by the following selection criteria:

- **Lepton Selection:**  $N(\mu^\pm) = 3, N(\mu^\mp) = 1,$
- **Fat-jet Selection:**  $N(J) = 2, 50 \text{ GeV} < m_J < 110 \text{ GeV}.$

All the two fat-jets in the final state are required to probe the heavy Higgs  $H$ .

In Figure 6, we show some variables of the same-sign trilepton signature after the pre-selection cuts. For the muon transverse momentum  $P_T(\mu)$  of the same-sign trilepton signature, it tends to be larger than that of the same-sign tetralepton signature for the corresponding benchmarks. This is because there are two muons

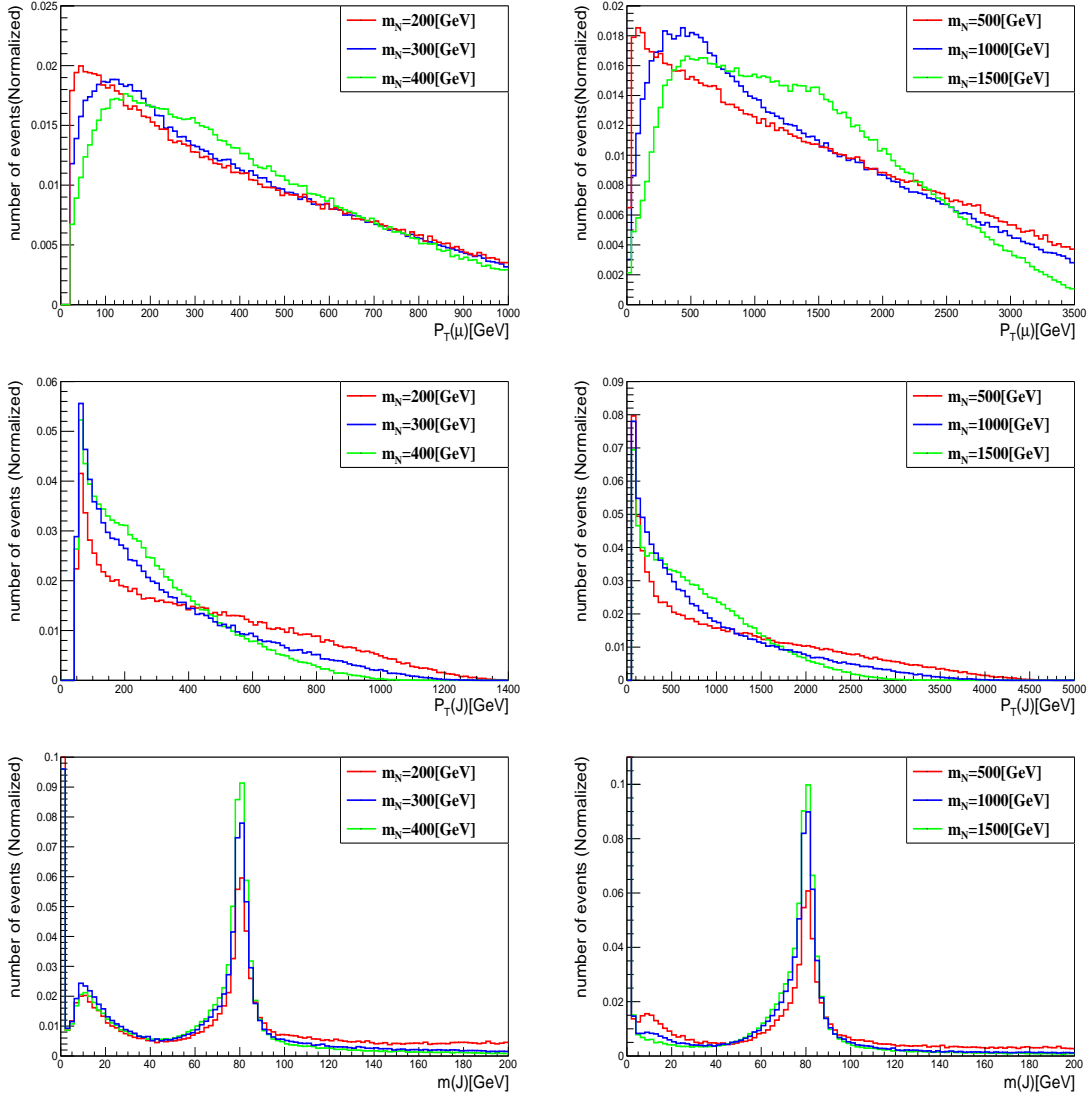


FIG. 6. Normalized distributions of muon transverse momentum  $P_T(\mu)$ , fat-jet transverse momentum  $P_T(J)$ , and invariant mass of fat-jet  $m_J$ . Left panels are the results of 3 TeV, and right panels are the results of 10 TeV. During the simulation of these plots, we have assumed the relation  $m_{Z'} = m_H = 3m_N$  for illustration.

coming from the direct decay of gauge boson  $Z' \rightarrow \mu^+ \mu^-$  in the trilepton signature, while the cascade decay of heavy neutrino  $N \rightarrow \mu^\pm J$  generates all muons in the tetralepton one. On the other hand, the fat-jet transverse momentum  $P_T(J)$  and invariant mass  $m_J$  of the same-sign trilepton signature are quite similar to those of the tetralepton signal, as they are all induced by the channel of  $N \rightarrow \mu^\pm J$ . We keep the same cut on  $m_J$  to select fat-jet from  $W$  decay.

In Table II, we show the results of the same-sign trilepton signature at the muon collider, which is also under the assumption of  $m_{Z'} = m_H = 3m_N$  and  $g' = 0.6$ . The after selection cuts cross sections at the 3

$\mu^+ \mu^- \rightarrow 3\mu^\pm \mu^\mp + 2J$		Pre-Selection (fb)	After Selection (fb)	Significance	5 $\sigma$ Luminosity (fb $^{-1}$ )
3 TeV	$m_N = 200$ GeV	3.20	1.73	149	4.82
	$m_N = 300$ GeV	3.95	2.61	189	3.19
	$m_N = 400$ GeV	4.56	3.03	206	2.75
10 TeV	$m_N = 500$ GeV	0.251	0.129	126	64.6
	$m_N = 1000$ GeV	0.353	0.229	175	36.4
	$m_N = 1500$ GeV	0.372	0.238	180	35.0

TABLE II. Same as Table I, but for the same-sign trilepton signature  $\mu^+ \mu^- \rightarrow 3\mu^\pm \mu^\mp + 2J$ .

TeV muon collider are 1.73 fb, 2.61 fb, and 3.03 fb for  $m_N = 200$  GeV, 300 GeV, and 400 GeV, respectively. With an integrated luminosity of 1 ab $^{-1}$ , the significance could reach 149, 189, and 206, accordingly. All these 3 TeV benchmarks can be discovered with less than 5 fb $^{-1}$  data. For the three benchmarks at the 10 TeV muon collider, the typical cross section after selection cuts is at the order of  $\mathcal{O}(0.1)$  fb. With 10 ab $^{-1}$  data, the significance of these 10 TeV benchmarks can also exceed 100. The benchmark with  $m_N = 500$  GeV, 1000 GeV, and 1500 GeV can be discovered at the 10 TeV muon collider with 64.6 fb $^{-1}$ , 36.4 fb $^{-1}$ , and 35.0 fb $^{-1}$  data. Compared to the same-sign tetralepton signal, the cross section of the same-sign trilepton signature is about two orders of magnitude larger for certain benchmarks. Therefore, this less exotic same-sign trilepton signature  $3\mu^\pm \mu^\mp + 2J$  is quite promising as the discovery channel of the heavy neutral lepton at the muon collider.

Within the same-sign trilepton signature, the three same-sign muons originate from different heavy resonances. One is from the direct decay  $Z' \rightarrow \mu^+ \mu^-$ , and the other two are from the decay  $N \rightarrow \mu^\pm J$ . In this section, we perform a combined analysis by minimizing

$$\chi^2_{NZ'} = \sum_{i,j,k} (m_{\mu_i^\pm J_j} - m_N)^2 + (m_{\mu_k^\pm \mu^\mp} - m_{Z'})^2, \quad (36)$$

to reconstruct the heavy neutral lepton and new gauge boson simultaneously. Although we assume  $m_{Z'} = m_H$  for illustration, this  $\chi^2_{NZ'}$  function is applicable for the scenario of  $m_{Z'} \neq m_H$ . The results are shown in the first two rows of Figure 7.

For the heavy Higgs, there are two viable pathways to reconstruct its mass. The first one is directly determined by the invariant mass of the two heavy neutral leptons  $m_{NN}$ , which originates from the decay mode  $H \rightarrow NN$ . Similar to the vanilla Higgs-strahlung process  $\ell^+ \ell^- \rightarrow Zh$ , the second approach is considering the recoil mass of the visible decay  $Z' \rightarrow \mu^+ \mu^-$

$$m_{\text{rec}}^2 = (\sqrt{s} - E_{\mu^+ \mu^-})^2 - p_{\mu^+ \mu^-}^2 = s - 2E_{\mu^+ \mu^-}\sqrt{s} + m_{\mu^+ \mu^-}^2, \quad (37)$$

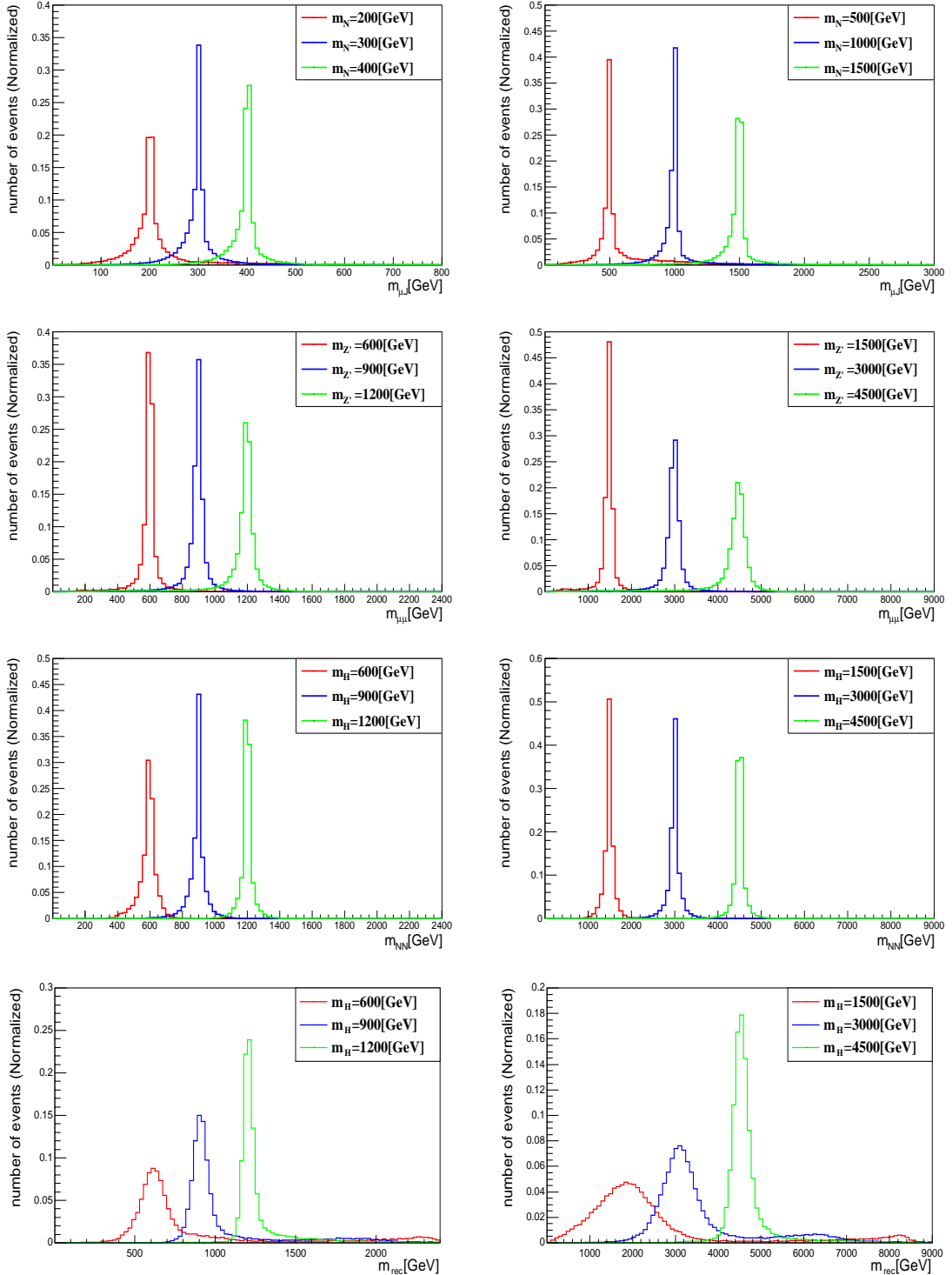


FIG. 7. Normalized distributions of invariant mass of muon and fat-jet  $m_{\mu J}$ , invariant mass of two opposite-sign muon  $m_{\mu\mu}$ , invariant mass of two reconstructed heavy neutral lepton  $m_{NN}$ , and recoil mass  $m_{rec}$ . Left panels are the results of 3 TeV, and right panels are the results of 10 TeV. The relation  $m_{Z'} = m_H = 3m_N$  is also assumed.

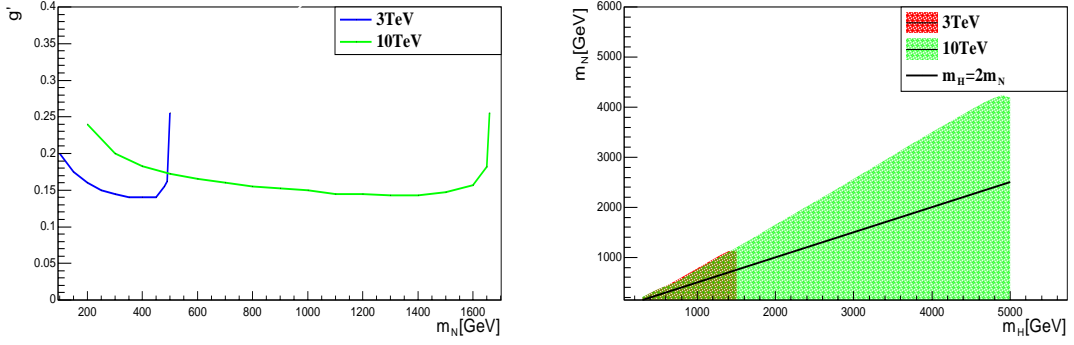


FIG. 8. Left: The  $5\sigma$  discovery region of the same-sign trilepton signature in the  $g' - m_N$  plane, where we fix  $m_{Z'} = m_H = 3m_N$ . Right: The  $5\sigma$  discovery region of the same-sign trilepton signature in the  $m_N - m_H$  plane, where we fix  $m_{Z'} = m_H$  and  $g' = 0.6$ .

where  $E_{\mu^+\mu^-}$ ,  $p_{\mu^+\mu^-}$ , and  $m_{\mu^+\mu^-}$  are the total energy, momentum and invariant mass of the opposite-sign muon pair  $\mu^+\mu^-$  from  $Z'$ . The reconstructed heavy Higgs mass via invariant mass  $m_{NN}$  and recoil mass  $m_{\text{rec}}$  are shown in the third and fourth row of Figure 7. According to Equation (37), the resolution of recoil mass heavily depends on the energy resolution of the muon. Because of the smaller energy detector resolution smearing at a lower muon energy [84], we find that the spread of recoil mass peak decreases as the heavy Higgs mass increases. In this way, the direct invariant mass  $m_{NN}$  is more precise than the recoil mass  $m_{\text{rec}}$  to determine the heavy Higgs mass at the TeV scale muon collider.

In the left panel of Figure 8, we depict the  $5\sigma$  discovery region of the same-sign trilepton signature. The 3 TeV muon collider could discover the region with  $g' \gtrsim 0.14$  for the electroweak scale heavy neutral lepton. Meanwhile, the 10 TeV is promising to discover heavy neutral lepton around the TeV scale when  $g' \gtrsim 0.15$ . We report that with a relatively large gauge coupling  $g' = 0.6$ , the same-sign trilepton signature actually could probe the off-shell decay region when  $m_H < 2m_N$ . In such area, the lepton number violation Higgs decay is dominated by the three-body channel  $H \rightarrow N^*N \rightarrow \mu^\pm W^\mp N \rightarrow \mu^\pm \mu^\pm JJ$  in the decoupling limit  $\sin \alpha = 0$ . Above approximately the  $m_N \gtrsim 0.8m_H$  region, the four-body decay channel  $H \rightarrow Z'^*Z'^* \rightarrow 4\ell$  ( $\ell = \mu, \tau$ ) with  $m_H = m_{Z'}$  becomes the dominant channel, which leads to the upper bounds of the same-sign trilepton signature.

## VII. CONCLUSION

After the spontaneous symmetry breaking, we have the new gauge boson  $Z'$  and heavy Higgs boson  $H$  in the  $U(1)$  gauged extension of the type-I seesaw mechanism. As the benchmark model, we consider the

currently less constrained  $U(1)_{L_\mu-L_\tau}$  symmetry. These new bosons can be produced through the heavy Higgs-strahlung process  $\mu^+\mu^- \rightarrow Z'H$  at the future muon collider, which typically reaches the maximum cross section near the threshold  $\sqrt{s} \sim m_{Z'} + m_H$ . In this way, the TeV scale muon collider is promising to detect these particles  $Z'$  and  $H$  also around the TeV scale.

Further decays of  $Z'$  and  $H$ , such as  $Z' \rightarrow NN/\mu^+\mu^-, H \rightarrow NN$ , lead to various novel signatures at the muon collider. In this paper, we investigate the same-sign tetralepton signature  $\mu^+\mu^- \rightarrow Z'H \rightarrow NN + NN \rightarrow 4\mu^\pm + 4J$  and the same-sign trilepton signature  $\mu^+\mu^- \rightarrow Z'H \rightarrow \mu^+\mu^- + NN \rightarrow 3\mu^\pm\mu^\mp + 2J$  at the 3 TeV and 10 TeV muon collider. These lepton number violation signatures have a quite clean background. With a relatively larger production cross section, we find that the 3 TeV muon collider is usually more promising than the 10 TeV one to detect heavy neutral lepton around the electroweak scale. Meanwhile, the 10 TeV muon collider could discover TeV-scale heavy neutral lepton mainly due to larger luminosity.

The same-sign tetralepton signature  $\mu^+\mu^- \rightarrow Z'H \rightarrow NN + NN \rightarrow 4\mu^\pm + 4J$  is the most novel one, which violates the lepton number by four units. We find that the muon collider could discover this novel signature when  $g' \gtrsim 0.4$ . With a much larger cross section, the same-sign trilepton signature  $\mu^+\mu^- \rightarrow Z'H \rightarrow \mu^+\mu^- + NN \rightarrow 3\mu^\pm\mu^\mp + 2J$  is more promising as the discovery channel, which could probe the region with  $g' \gtrsim 0.15$ . Limited by the decay  $Z' \rightarrow NN$ , the same-sign tetralepton signature is only viable within the regime of  $m_{Z'} > 2m_N$ . On the other hand, through the three-body decay  $H \rightarrow N^*N \rightarrow \mu^\pm W^\mp N$  in the decoupling limit  $\sin \alpha = 0$ , the same-sign trilepton signature could also test the off-shell decay region when  $m_H < 2m_N$ .

It should be mentioned that our results are based on the simplified scenario with  $m_{Z'} = m_H$ . The more general scenario with  $m_{Z'} \sim m_H$  leads to similar results, because the production cross section will not change too much. However, there are two exception regimes. One is the light new gauge boson scenario with  $2m_{Z'} \ll m_H$ , where the branching ratio of  $H \rightarrow NN$  is suppressed. The other one is the threshold region  $\sqrt{s} \sim m_{Z'} + m_H$  with  $m_{Z'} \gg m_H$ , where the production cross section could be largely enhanced. The most general scenario with  $m_{Z'} \neq m_H$  can be easily confirmed by comparing the invariant mass  $m_{\mu^+\mu^-}$  and recoil mass  $m_{\text{rec}}$  of the muon pair from  $Z' \rightarrow \mu^+\mu^-$ .

In principle, our results are also applicable to the  $U(1)_{B-L}$  symmetry. However, under the stringent constraints from dilepton search  $Z' \rightarrow \ell^+\ell^-$ , the promising regions of these novel signatures at the 3 TeV muon collider are already excluded by the current limit  $m_{Z'} > 5.1$  TeV. At the 10 TeV muon collider, there is still a viable region with  $m_H < m_{Z'}$  and  $m_H + m_{Z'} < 10$  TeV. The larger parameter space of  $U(1)_{B-L}$  can be tested at a muon collider with higher collision energy, such as the 30 TeV option.

### ACKNOWLEDGMENTS

This work is supported by the National Natural Science Foundation of China under Grant No. 12505112, Natural Science Foundation of Shandong Province under Grant No. ZR2022MA056 and ZR2024QA138, State Key Laboratory of Dark Matter Physics, and University of Jinan Disciplinary Cross-Convergence Construction Project 2024 (XKJC-202404).

---

[1] Y. Fukuda *et al.* [Super-Kamiokande], Phys. Rev. Lett. **81**, 1562-1567 (1998) [arXiv:hep-ex/9807003 [hep-ex]].

[2] Q. R. Ahmad *et al.* [SNO], Phys. Rev. Lett. **89**, 011301 (2002) [arXiv:nucl-ex/0204008 [nucl-ex]].

[3] F. P. An *et al.* [Daya Bay], Phys. Rev. Lett. **108**, 171803 (2012) [arXiv:1203.1669 [hep-ex]].

[4] P. Minkowski, Phys. Lett. B **67**, 421-428 (1977)

[5] R. N. Mohapatra and G. Senjanovic, Phys. Rev. Lett. **44**, 912 (1980)

[6] J. Schechter and J. W. F. Valle, Phys. Rev. D **22**, 2227 (1980)

[7] J. Schechter and J. W. F. Valle, Phys. Rev. D **25**, 774 (1982)

[8] T. Han and B. Zhang, Phys. Rev. Lett. **97**, 171804 (2006) [arXiv:hep-ph/0604064 [hep-ph]].

[9] F. F. Deppisch, P. S. Bhupal Dev and A. Pilaftsis, New J. Phys. **17**, no.7, 075019 (2015) [arXiv:1502.06541 [hep-ph]].

[10] Y. Cai, T. Han, T. Li and R. Ruiz, Front. in Phys. **6**, 40 (2018) [arXiv:1711.02180 [hep-ph]].

[11] G. Aad *et al.* [ATLAS], JHEP **10**, 265 (2019) [arXiv:1905.09787 [hep-ex]].

[12] G. Aad *et al.* [ATLAS], Phys. Rev. Lett. **131**, no.6, 061803 (2023) [arXiv:2204.11988 [hep-ex]].

[13] A. Tumasyan *et al.* [CMS], JHEP **07**, 081 (2022) [arXiv:2201.05578 [hep-ex]].

[14] A. Hayrapetyan *et al.* [CMS], JHEP **03**, 105 (2024) [arXiv:2312.07484 [hep-ex]].

[15] A. Hayrapetyan *et al.* [CMS], JHEP **06**, 123 (2024) [arXiv:2403.00100 [hep-ex]].

[16] A. M. Abdullahi, P. B. Alzas, B. Batell, J. Beacham, A. Boyarsky, S. Carballo, A. Chatterjee, J. I. Crespo-Adan, F. F. Deppisch and A. De Roeck, *et al.* J. Phys. G **50**, no.2, 020501 (2023) [arXiv:2203.08039 [hep-ph]].

[17] J. C. Pati and A. Salam, Phys. Rev. D **10**, 275-289 (1974) [erratum: Phys. Rev. D **11**, 703-703 (1975)]

[18] R. N. Mohapatra and J. C. Pati, Phys. Rev. D **11**, 2558 (1975)

[19] G. Senjanovic and R. N. Mohapatra, Phys. Rev. D **12**, 1502 (1975)

[20] A. Davidson, Phys. Rev. D **20**, 776 (1979)

[21] R. E. Marshak and R. N. Mohapatra, Phys. Lett. B **91**, 222-224 (1980)

[22] R. N. Mohapatra and R. E. Marshak, Phys. Rev. Lett. **44**, 1316-1319 (1980) [erratum: Phys. Rev. Lett. **44**, 1643 (1980)]

[23] K. Huitu, S. Khalil, H. Okada and S. K. Rai, Phys. Rev. Lett. **101**, 181802 (2008) [arXiv:0803.2799 [hep-ph]].

[24] L. Basso, A. Belyaev, S. Moretti and C. H. Shepherd-Themistocleous, Phys. Rev. D **80**, 055030 (2009) [arXiv:0812.4313 [hep-ph]].

[25] T. Han, I. Lewis, R. Ruiz and Z. g. Si, Phys. Rev. D **87**, no.3, 035011 (2013) [erratum: Phys. Rev. D **87**, no.3, 039906 (2013)] [arXiv:1211.6447 [hep-ph]].

[26] A. Maiezza, M. Nemevšek and F. Nesti, Phys. Rev. Lett. **115**, 081802 (2015) [arXiv:1503.06834 [hep-ph]].

[27] M. Nemevšek, F. Nesti and G. Popara, Phys. Rev. D **97**, no.11, 115018 (2018) [arXiv:1801.05813 [hep-ph]].

[28] G. Aad *et al.* [ATLAS], Phys. Lett. B **796**, 68-87 (2019) [arXiv:1903.06248 [hep-ex]].

[29] G. Aad *et al.* [ATLAS], Eur. Phys. J. C **83**, no.12, 1164 (2023) [arXiv:2304.09553 [hep-ex]].

[30] A. Tumasyan *et al.* [CMS], JHEP **04**, 047 (2022) [arXiv:2112.03949 [hep-ex]].

[31] A. Tumasyan *et al.* [CMS], JHEP **11**, 181 (2023) [arXiv:2307.06959 [hep-ex]].

[32] X. G. He, G. C. Joshi, H. Lew and R. R. Volkas, Phys. Rev. D **43**, 22-24 (1991)

[33] R. Foot, X. G. He, H. Lew and R. R. Volkas, Phys. Rev. D **50**, 4571-4580 (1994) [arXiv:hep-ph/9401250 [hep-ph]].

[34] G. Aad *et al.* [ATLAS], JHEP **07**, 090 (2023) [arXiv:2301.09342 [hep-ex]].

[35] G. Aad *et al.* [ATLAS], Phys. Rev. D **110**, no.7, 072008 (2024) [arXiv:2402.15212 [hep-ex]].

[36] G. y. Huang, F. S. Queiroz and W. Rodejohann, Phys. Rev. D **103**, no.9, 095005 (2021) [arXiv:2101.04956 [hep-ph]].

[37] J. Sun, F. Huang and X. G. He, Phys. Lett. B **845**, 138121 (2023)

[38] A. Dasgupta, P. S. B. Dev, T. Han, R. Padhan, S. Wang and K. Xie, JHEP **12**, 011 (2023) [arXiv:2308.12804 [hep-ph]].

[39] I. Chakraborty, H. Roy and T. Srivastava, Eur. Phys. J. C **83**, no.4, 280 (2023) [arXiv:2206.07037 [hep-ph]].

[40] K. Mekała, J. Reuter and A. F. Żarnecki, Phys. Lett. B **841**, 137945 (2023) [arXiv:2301.02602 [hep-ph]].

[41] T. H. Kwok, L. Li, T. Liu and A. Rock, Phys. Rev. D **110**, no.7, 075009 (2024) [arXiv:2301.05177 [hep-ph]].

[42] P. Li, Z. Liu and K. F. Lyu, JHEP **03**, 231 (2023) [arXiv:2301.07117 [hep-ph]].

[43] Z. Wang, X. H. Yang and X. Y. Zhang, Phys. Lett. B **853**, 138643 (2024) [arXiv:2311.15166 [hep-ph]].

[44] Q. H. Cao, K. Cheng and Y. Liu, Phys. Rev. Lett. **134**, no.2, 021801 (2025) [arXiv:2403.06561 [hep-ph]].

[45] D. Barducci and A. Dondarini, JHEP **10**, 165 (2024) [arXiv:2404.09609 [hep-ph]].

[46] M. Frigerio and N. Vignaroli, JHEP **04**, 008 (2025) [arXiv:2409.02721 [hep-ph]].

[47] N. Vignaroli, [arXiv:2507.01130 [hep-ph]].

[48] T. Li, C. Y. Yao and M. Yuan, JHEP **09**, 131 (2023) [arXiv:2306.17368 [hep-ph]].

[49] O. Mikulenko and M. Marinichenko, JHEP **01**, 032 (2024) [arXiv:2309.16837 [hep-ph]].

[50] P. Dehghani, M. Frank and B. Fuks, [arXiv:2506.06159 [hep-ph]].

[51] E. Antonov, A. Drutskoy and M. Dubinin, JETP Lett. **118**, no.7, 461-469 (2023) [arXiv:2308.02240 [hep-ph]].

[52] R. Jiang, T. Yang, S. Qian, Y. Ban, J. Li, Z. You and Q. Li, Phys. Rev. D **109**, no.3, 035020 (2024) [arXiv:2304.04483 [hep-ph]].

[53] C. H. de Lima, D. McKeen, J. N. Ng, M. Shamma and D. Tuckler, Phys. Rev. D **111**, no.7, 075002 (2025) [arXiv:2411.15303 [hep-ph]].

- [54] S. Bhattacharya, S. Datta and A. Sarkar, [arXiv:2505.20936 [hep-ph]].
- [55] W. Liu, K. P. Xie and Z. Yi, Phys. Rev. D **105**, no.9, 095034 (2022) [arXiv:2109.15087 [hep-ph]].
- [56] R. Y. He, J. Q. Huang, J. Y. Xu, F. X. Yang, Z. L. Han and F. L. Shao, Chin. Phys. C **48**, no.9, 093102 (2024) [arXiv:2401.14687 [hep-ph]].
- [57] Q. Bi, J. Guo, J. Liu, Y. Luo and X. P. Wang, Phys. Rev. D **111**, no.7, 075001 (2025) [arXiv:2409.17243 [hep-ph]].
- [58] M. B. Marcos, A. de Giorgi, L. Merlo and J. L. Tastet, SciPost Phys. **18**, 084 (2025) [arXiv:2407.14970 [hep-ph]].
- [59] A. Batra, P. Bharadwaj, S. Mandal, R. Srivastava and J. W. F. Valle, Phys. Lett. B **860**, 139204 (2025) [arXiv:2304.06080 [hep-ph]].
- [60] F. X. Yang, F. L. Shao, Z. L. Han, F. Huang, Y. Jin and H. Li, JHEP **09**, 200 (2025) [arXiv:2505.07331 [hep-ph]].
- [61] A. Das, T. Nomura and K. Yagyu, [arXiv:2512.03302 [hep-ph]].
- [62] W. Kilian, M. Kramer and P. M. Zerwas, Phys. Lett. B **373**, 135-140 (1996) [arXiv:hep-ph/9512355 [hep-ph]].
- [63] M. Carena and H. E. Haber, Prog. Part. Nucl. Phys. **50**, 63-152 (2003) [arXiv:hep-ph/0208209 [hep-ph]].
- [64] P. Andreetto, N. Bartosik, L. Buonincontri, D. Calzolari, V. Candelise, M. Casarsa, L. Castelli, M. Chiesa, A. Colaleo and G. Da Molin, *et al.* Eur. Phys. J. C **85**, no.3, 221 (2025) [arXiv:2405.19314 [hep-ex]].
- [65] L. Basso, S. Moretti and G. M. Pruna, Eur. Phys. J. C **71**, 1724 (2011) [arXiv:1012.0167 [hep-ph]].
- [66] A. Das, T. Nomura and T. Shimomura, Eur. Phys. J. C **83**, no.9, 786 (2023) [arXiv:2212.11674 [hep-ph]].
- [67] S. K.A., A. Das, G. Lambiase, T. Nomura and Y. Orikasa, Eur. Phys. J. C **84**, no.11, 1224 (2024) [arXiv:2308.14483 [hep-ph]].
- [68] T. Nomura and K. Yagyu, Phys. Rev. D **111**, no.1, 015034 (2025) [arXiv:2407.20742 [hep-ph]].
- [69] G. Arcadi, T. Hugle and F. S. Queiroz, Phys. Lett. B **784**, 151-158 (2018) [arXiv:1803.05723 [hep-ph]].
- [70] T. Hapitas, D. Tuckler and Y. Zhang, Phys. Rev. D **105**, no.1, 016014 (2022) [arXiv:2108.12440 [hep-ph]].
- [71] X. Yin, H. Li, Y. Jin, Z. Han and Z. Lu, Chin. Phys. C **46**, no.5, 053106 (2022) [arXiv:2112.13975 [hep-ph]].
- [72] Z. Lu, H. Li, Z. L. Han, Z. G. Si and L. Zhao, Sci. China Phys. Mech. Astron. **67**, no.3, 231012 (2024) [arXiv:2312.17427 [hep-ph]].
- [73] T. Nomura and T. Shimomura, Eur. Phys. J. C **81**, no.4, 297 (2021) [arXiv:2012.13049 [hep-ph]].
- [74] S. D. Lane, I. M. Lewis and M. Sullivan, Phys. Rev. D **110**, no.5, 5 (2024) [arXiv:2403.18003 [hep-ph]].
- [75] K. Asai, K. Hamaguchi, N. Nagata, S. Y. Tseng and K. Tsumura, Phys. Rev. D **99**, no.5, 055029 (2019) [arXiv:1811.07571 [hep-ph]].
- [76] C. Accettura, D. Adams, R. Agarwal, C. Ahdida, C. Aimè, N. Amapane, D. Amorim, P. Andreetto, F. Anulli and R. Appleby, *et al.* Eur. Phys. J. C **83**, no.9, 864 (2023) [erratum: Eur. Phys. J. C **84**, no.1, 36 (2024)] [arXiv:2303.08533 [physics.acc-ph]].
- [77] C. Accettura *et al.* [International Muon Collider], [arXiv:2504.21417 [physics.acc-ph]].
- [78] A. Alloul, N. D. Christensen, C. Degrande, C. Duhr and B. Fuks, Comput. Phys. Commun. **185**, 2250-2300 (2014) [arXiv:1310.1921 [hep-ph]].

- [79] J. Alwall, R. Frederix, S. Frixione, V. Hirschi, F. Maltoni, O. Mattelaer, H. S. Shao, T. Stelzer, P. Torrielli and M. Zaro, JHEP **07**, 079 (2014) [arXiv:1405.0301 [hep-ph]].
- [80] T. Sjöstrand, S. Ask, J. R. Christiansen, R. Corke, N. Desai, P. Ilten, S. Mrenna, S. Prestel, C. O. Rasmussen and P. Z. Skands, Comput. Phys. Commun. **191**, 159-177 (2015) [arXiv:1410.3012 [hep-ph]].
- [81] J. de Favereau *et al.* [DELPHES 3], JHEP **02**, 057 (2014) [arXiv:1307.6346 [hep-ex]].
- [82] M. Boronat, J. Fuster, I. Garcia, E. Ros and M. Vos, Phys. Lett. B **750**, 95-99 (2015) [arXiv:1404.4294 [hep-ex]].
- [83] G. Cowan, K. Cranmer, E. Gross and O. Vitells, Eur. Phys. J. C **71**, 1554 (2011) [erratum: Eur. Phys. J. C **73**, 2501 (2013)] [arXiv:1007.1727 [physics.data-an]].
- [84] N. Chakrabarty, T. Han, Z. Liu and B. Mukhopadhyaya, Phys. Rev. D **91**, no.1, 015008 (2015) [arXiv:1408.5912 [hep-ph]].